M.SNEHA PRIYA, G. JAMUNA RANI / International Journal of Engineering Research and Applications (IJERA) ISSN: 2248-9622 www.ijera.com
Vol. 2, Issue 3, May-Jun 2012, pp.2133-2144

PERIODIC FLOW SIMULATION AND HEAT TRANSFER ANALYSIS USING COMPUTATIONAL FLUID DYNAMICS (CFD)

***M.SNEHA PRIYA, **G. JAMUNA RANI**
* (Department of Mechanical Engineering, koneru lakshmai University, Guntur)
**(Department of Mechanical Engineering, koneru lakshmai University, Guntur)

ABSTRACT
Many heat transfer applications, such as steam generators in a boiler or air cooling in the coil of an air conditioner, can be modelled in a bank of tubes containing a flowing fluid at one temperature that is immersed in a second fluid in a cross flow at different temperature. CFD simulations are a useful tool for understanding flow and heat transfer principles as well as for modelling these type of geometries Both fluids considered in the present study are water, and flow is classified as laminar and steady, with Reynolds number between 100-600.The mass flow rate of the cross flow and diameter is been varied (such as 0.05, 0.1, 0.15, 0.20, 0.25, 0.30 kg/sec) and the models are used to predict the flow and temperature fields that result from convective heat transfer. Due to symmetry of the tube bank and the periodicity of the flow inherent in the tube bank geometry, only a portion of the geometry will be modelled and with symmetry applied to the outer boundaries. The inflow boundary will be redefined as a periodic zone and the outflow boundary is defined as the shadow. In the present paper tubes of different diameters and different mass flow rates are considered to examine the optimal flow distribution. Further the problem has been subjected to effect of materials used for tubes manufacturing on heat transfer rate. Materials

considered are aluminium which is used widely for manufacture of tubes, copper and alloys.
Keywords: heat transfer, heat exchangers, mass flow rate, Nusselt number, periodic flow.

I INTRODUCTION
Many industrial applications, such as steam generation in a boiler, air cooling in the coil of air conditioner and different type of heat exchangers uses tube banks to accomplish a desired total heat transfer.

The system considered for the present problem, consisted bank of tubes containing a flowing fluid at one temperature that is immersed in a second fluid in cross flow at a different temperature. Both fluids are water, and the flow is classified as laminar and steady, with a Reynolds number of approximately 100.The mass flow rate of cross flow is known, and the model is used to predict the flow and temperature fields that result from convective heat transfer due to the fluid flowing over tubes.

The figure depicts the frequently used tube banks in staggered arrangements. The situation is characterized by repetition of an identical module shown as transverse tubes. Due to symmetry of the tube bank, and the periodicity of the flow inherent in the tube geometry, only a portion of the geometry will be modelled as two dimensional periods' heat flows with symmetry applied to the outer boundaries.

II CFD MODELLING OF A PERIODIC MODEL
- Creating physical domain and meshing
- Creating periodic zones
- Set the material properties and imposing boundary conditions
- Calculating the solutions using segregated solver.

III MODELLING DETAILS AND MESHING

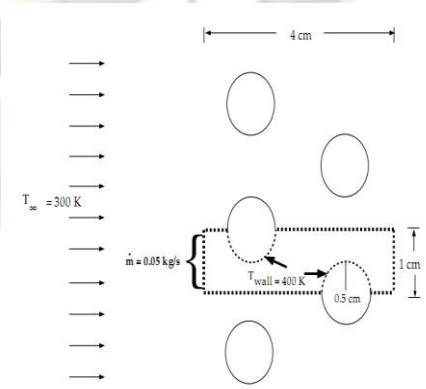

Figure 1: Schematic of the problem

The modelling and meshing package used is GAMBIT. The geometry consists of a periodic inlet and outlet boundaries, tube walls. The bank consists of uniformly spaced tubes with a diameter D, which are staggered in the direction of cross flow. Their centres are separated by a distance of 2cm in x-direction and 1 cm in y-direction.

The periodic domain shown by dashed lines in fig1 .is modelled for different tube diameter viz., D=0.8cm, 1.0cm, 1.2cm and 1.4cm while keeping the same dimensions in the x and y direction. The entire domain is meshed using a successive ratio scheme with quadrilateral cells. Then the mesh is exported to FLUENT where the periodic zones are created as the inflow boundary is redefined as a periodic zone and the outer flow boundary defined as its shadow, and to set physical data, boundary condition. The resulting mesh for four models is shown in fig 2.

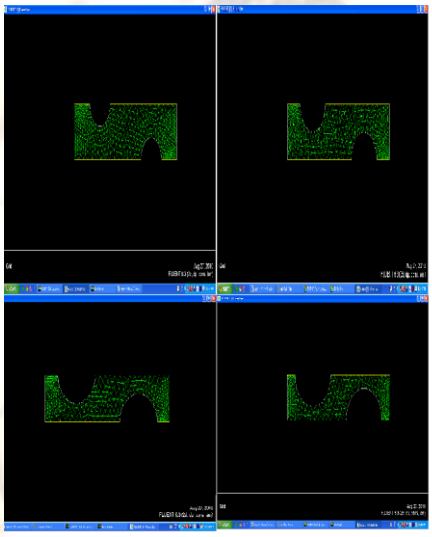

Fig 2 Mesh for the periodic tube of diameters 0.8, 1.0, 1.2, 1.4cm

The amount of cells, faces, nodes created while meshing for each domain is tabulated as follow:

Diameter (D)	Cells	Faces	Nodes
0.8cm	1921	3942	2052
1.0cm	1510	3115	1636
1.2cm	1787	3689	1933
1.4cm	1545	3212	1698

Table 1 Mesh Details

IV MATERIAL PROPERTIES AND BOUNDARY CONDITIONS

The material properties of working fluid (water) flowing over tube bank at bulk temperature of 300K, are:

$\rho = 998.2 kg/m^3$
$\mu = 0.001003 kg/m\text{-}s$
$C_p = 4182$ J/kg-k
K= 0.6 W/m-k

The boundary conditions applied on physical domain are as followed

Boundary	Assigned as
Inlet	Periodic
Outlet	Periodic
Tube walls	Wall
Outer walls	Symmetry

Table 2: Boundary conditions assigned in FLUENT

Fluid flow is one of the important characteristic of a tube bank. It is strongly effects the heat transfer process of a periodic domain and its overall performance. In this paper, different mass flow rates at free stream temperature, 300Kwere used and the wall temperature of the tube which was treated as heated section was set at 400K as periodic boundary conditions for each model which are tabulated as follows:

Tube diameter(D) (cm)	Periodic condition (Kg/s)
0.8	m=0.05-0.30
1.0	m=0.05,0.30
1.2	m=0.05-0.30
1.4	m=0.05-0.30

Table 3: Mass flow rates for different tube diameter

The wall temperature of the tube which was treated as heated section was set at 400k.

V SOLUTIONUSING SEGREGATE SOLVER:

The computational domain was solved using the solver settings as segregated, implicit, two-dimensional and steady state condition. The numerical simulation of the Navier Stokes equations, which governs the fluid flow and heat transfer, make use of the finite control volume method. CFD solved for temperature, pressure and flow velocity at every cell. Heat transfer was modelled through the energy equation. The simulation process was performed until the convergence and an accurate balance of mass and energy were achieved. The solution process is iterative, with each iteration in a steady state problem. There are two main iteration parameters to be set before commencing with the simulation. The under-relaxation factor determines the solution adjustment for each iteration; the residual cut off value determines when the iteration process can be terminated. The under-relaxation factor is an arbitrary number that determines the solution adjustment between two iterations; a high factor will result in a large adjustment and will result in a fast convergence, if the system is stable. In a less stable or particularly nonlinear system, for example in some turbulent flow or high- Rayleigh-number natural convection cases, a high under-relaxation may lead to divergence, an increase in error. It is therefore necessary to adjust the under- relaxation factor specifically to the system for which a solution is to be found. Lowering the under-relaxation factor in these unstable systems will lead to a smaller step change between the iterations,

leading to less adjustment in each step. This slows down the iterations process but decreases the chance for divergence of the residual values. The second parameter, the residual value, determines when a solution is converged. The residual value (a difference between the current and former solution value) is taken as a measure for convergence. In a infinite precision process the residuals will go to zero as the process converges. On actual computers the residuals decay to a certain small value (round-off) and then stop changing. This decay may be up to six orders of magnitude for single precision computations. By setting the upper limit of the residual values the 'cut-off' value for convergence is set. When the set value is reached the process is considered to have reached its 'round-off' value and the iteration process is stopped. Finally the under-relaxation factors and the residual cut-off values are set. Under- relaxation factors were set slightly below their default values to ensure stable convergence. Residual values were kept at their default values, $1.0e^{-6}$ for the energy residual, $1.0e^{-3}$ for all others, continuity, and velocities. The residual cut-off value for the energy balance is lower because it tends to be less stable than the other balances; the lower residual cut-off ensures that the energy solution has the same accuracy as the other values.

VI RESULTS AND DISCUSSIONS

I. Variation of static pressure for different tube diameter and mass flow rate

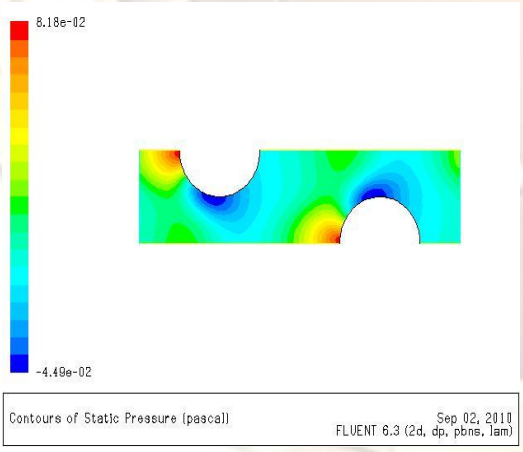

Figure 3 contours of static pressure, D=0.8cm m=0.05kg/s

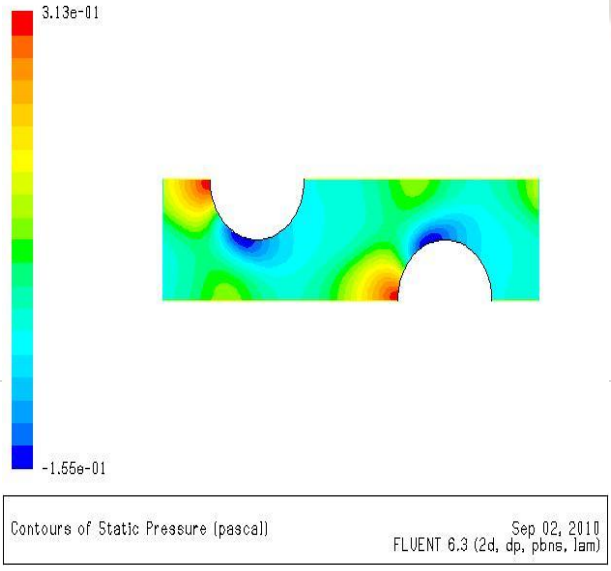

Figure 4 contours of static pressure, D=0.8cm m=0.10kg/s

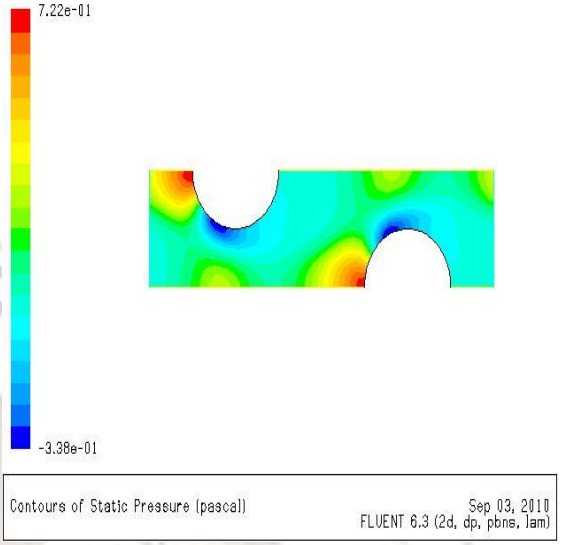

Figure 5 contours of static pressure, D=0.8cm m=0.15kg/s

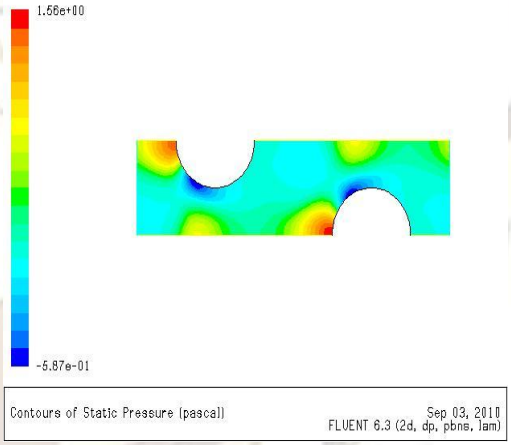

Figure 6 contours of static pressure, D=0.8cm m=0.20kg/s

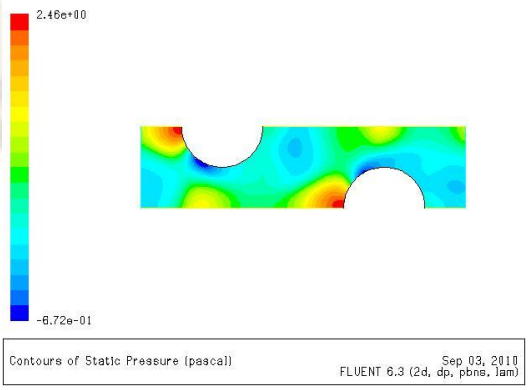

Figure 7 contours of static pressure, D=0.8cm m=0.25kg/s

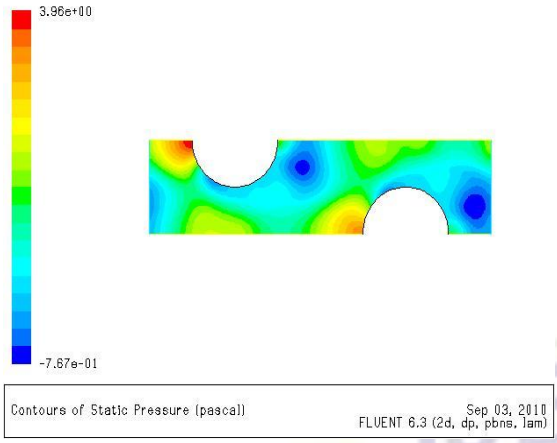

Figure 8 contours of static pressure, D=0.8cm m=0.30kg/s

The pressure contours are displayed in figures 3-8 do not include the linear pressure gradient computed by solver, thus the contours are periodic at the inflow and outflow boundaries. The figures reveal that the static pressure exerts at stagnation point differ mass flow rate have significant variation. It can be seen from fig 5.1, 5.2 the pressure at the stagnation point have almost similar magnitude in both cases while the flow past the tube the pressure varies drastically from one mass flow rate to the other mass flow rate. From fig 5.3 it can be observed, the pressure at stagnation point as well as the flow past the tube surface varies relatively more as compared to the previous geometries due to increase in tube diameter. Finally, it can be concluded that by changing the tube diameter and mass flow rate the pressure drop increases. Similarly, we have applied the same procedure for different diameters.

II Variation of static temperature for different tube diameter and mass flow rate

Figure 9 contours of static temperature, D=0.8cm m=0.05kg/s

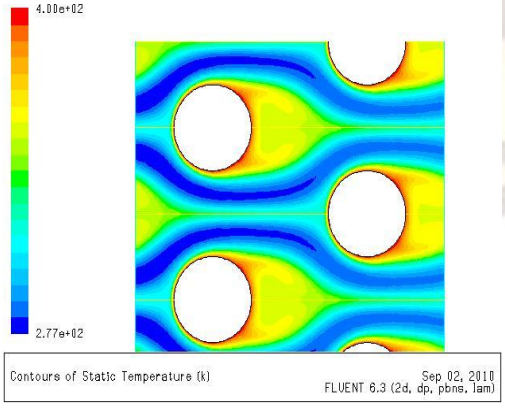

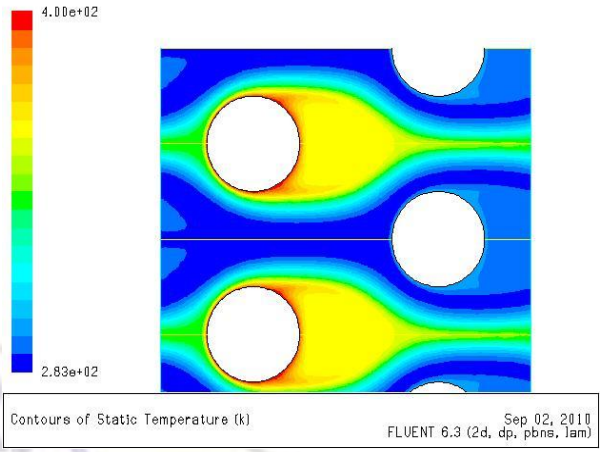

Figure 10 contours of static temperature, D=0.8cm m=0.10kg/s

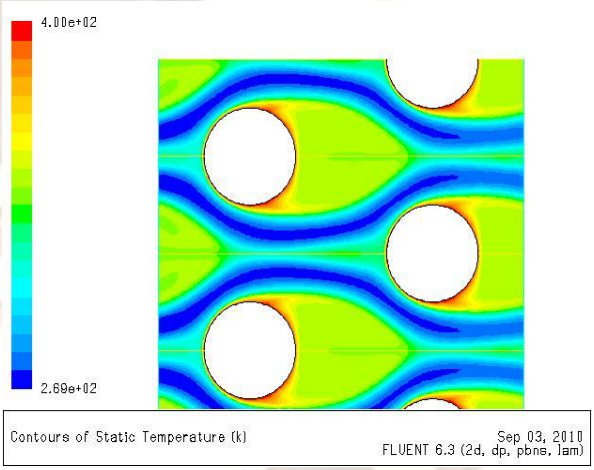

Figure 11 contours of static temperature, D=0.8 cm=0.15 kg/s

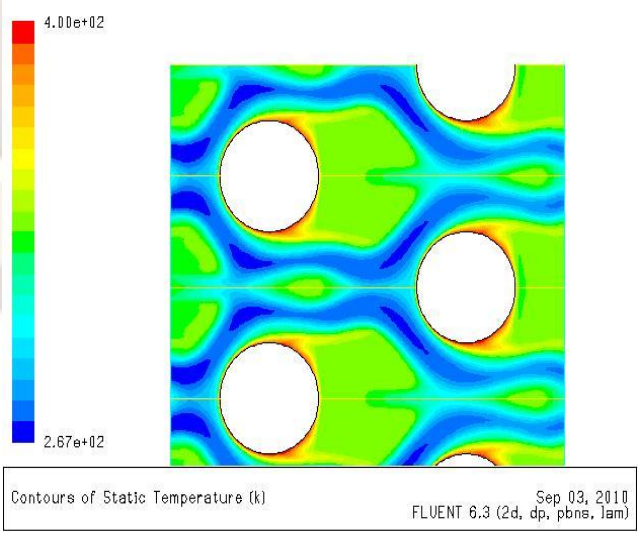

Figure 12 contours of static temperature, D=0.8 cm=0.20 kg/s

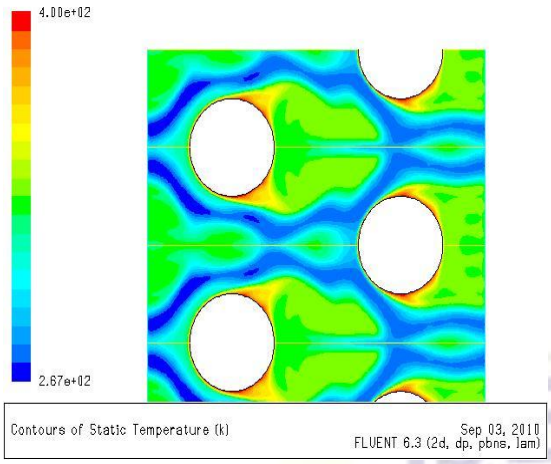

Figure 13 contours of static temperature, D=0.8cm=0.25 kg/s

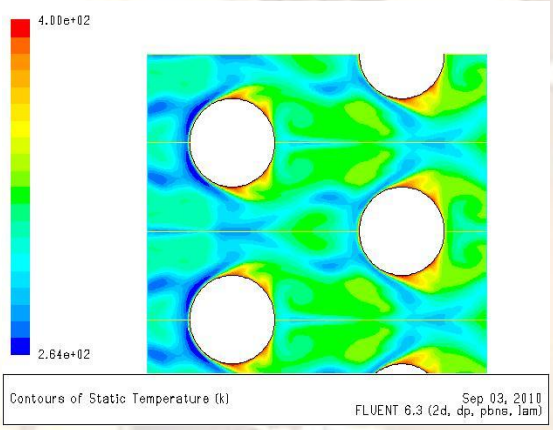

Figure 14 contours of static temperature, D=0.8cm=0.30 kg/s

The contours displayed in fig. 9-14 reveal the temperature increases in the fluid due to heat transfer from the tubes. The hotter fluid is confined to the near-wall and wake regions, while a narrow stream of cooler fluid is convected through the tube bank. The consequences of different mass flow rates to the fluid temperature distribution are shown in the above said figures. It can be seen that higher heat flow rate was obtained from low mass flow rates. The temperature scale is similar, when compared to one model to other three models for all mass flow rates. Similar procedure is repeated for other diameters.

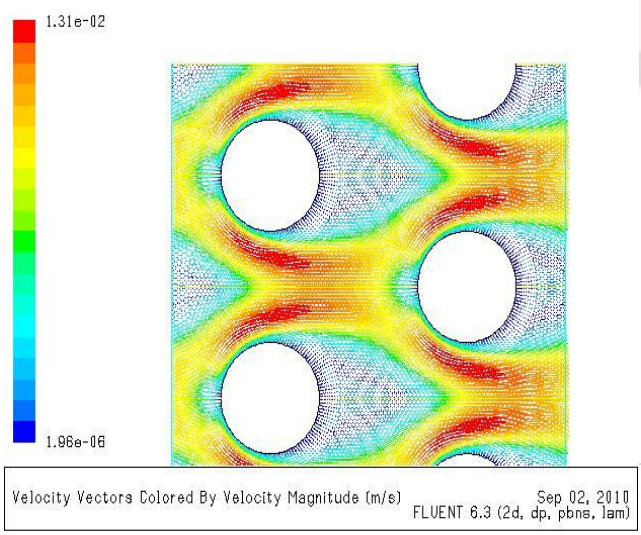

III Velocity vector for different tube diameters and mass flow rates:

Figure 15velocity vector, D=0.8cm=0.05 kg/s

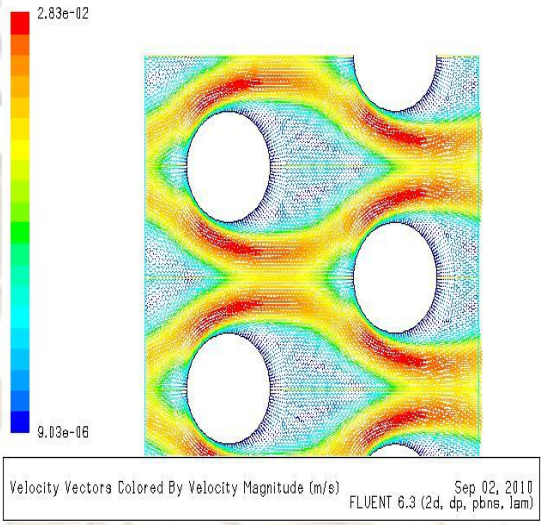

Figure 16 velocity vector, D=0.8cm=0.10 kg/s

.

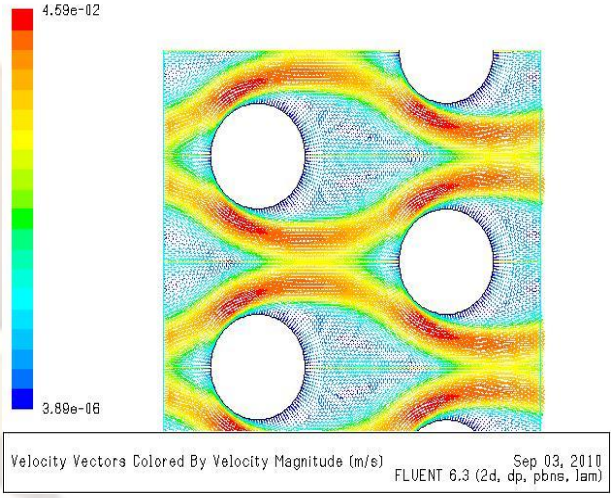

Figure 17 velocity vector, D=0.8cm=0.15kg/s

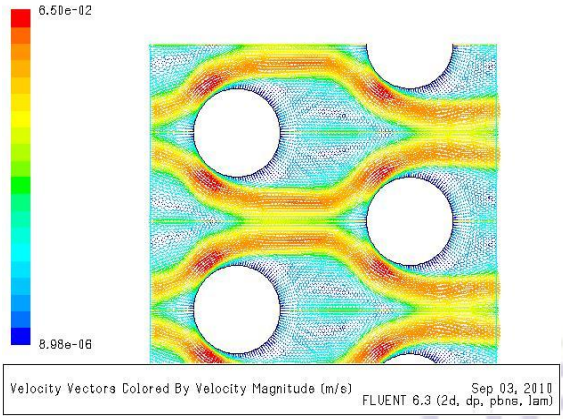

Figure 18 velocity vector, D=0.8 cm=0.120kg/s

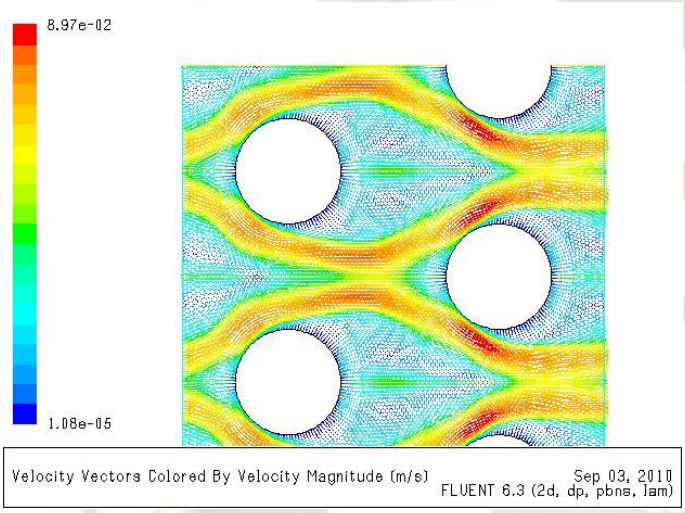

Figure 19 velocity vectors, D=0.8cm m=0.25kg/s

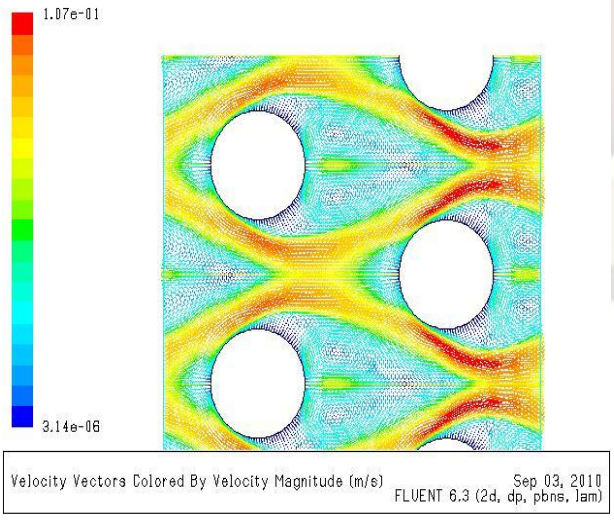

Figure 20 velocity vectors, D=0.8cm m=0.30kg/

When the fluid through the bank of tubes the maximum velocity occur at either the transverse plane or the diagonal plane where the flow area is minimum. The velocity vectors displayed in fig 5.7, 5.8, 5.9 reveal that the numerical results show very low velocity values adjacent to the tube surface. In the regimes between the tubes i.e., at the transverse plane the maximum velocity was occurred:

Since

$S_D = [S_L^2 + (S_r/2)^2]^{0.5} > S_r + D/2,$

The figures clearly show the boundary layer development along with the tube surface. It can be observed that the boundary layer detaches from the surface early due to less momentum of fluid in laminar flow, since the position of the separation point is highly depends on the Reynolds number. Finally, it can be observed from all the velocity vector diagrams, if the mass flow rate increased the velocity also increases and narrow stream of maximum velocity fluid through the tube bank

IV Static Pressure Variation in y-axis for different tube diameters and mass flow rates:

Figure 21 static pressure D=0.08cm, m=0.05kg/s

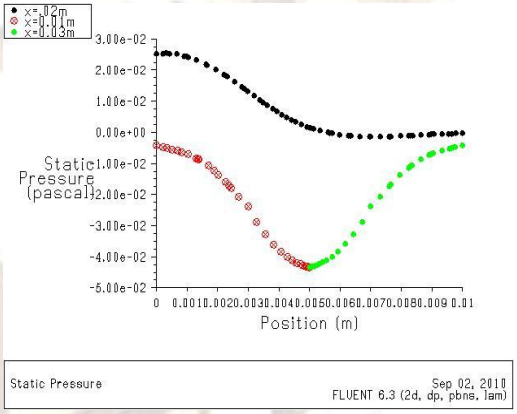

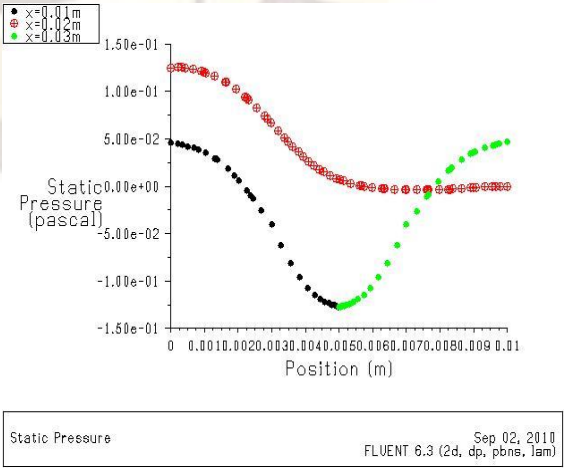

Figure 22 static pressure D=0.08cm, m=0.10kg/s

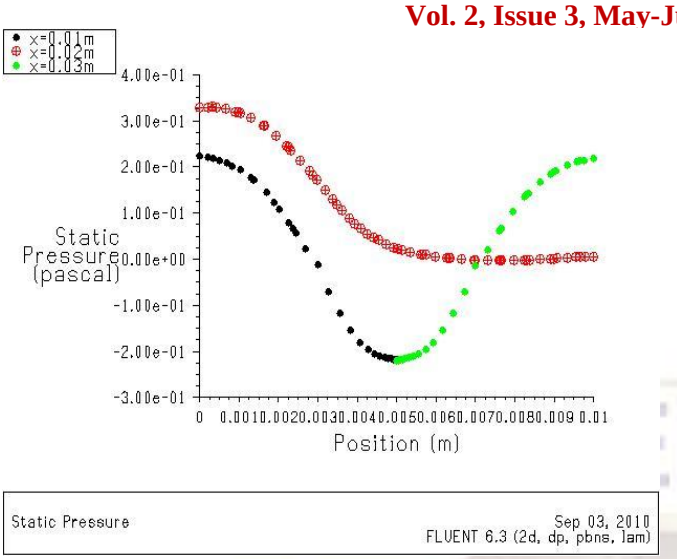

Figure 23 static pressure D=0.08cm, m=0.15kg/s

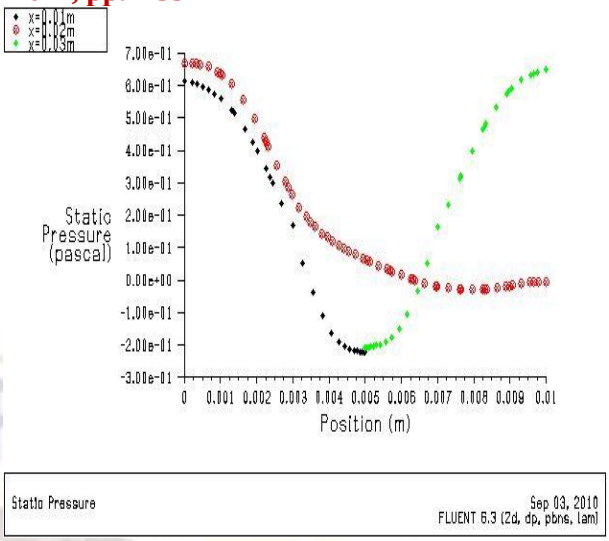

Figure 25 static pressure D=0.08cm, m=0.25kg/s

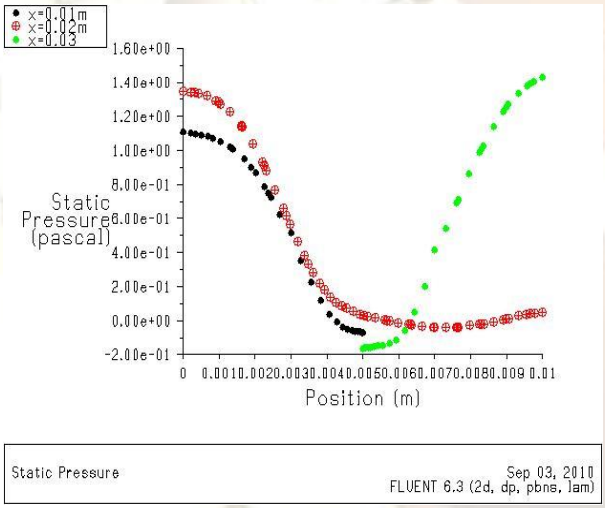

Figure 24 static pressure D=0.08cm, m=0.20kg/s

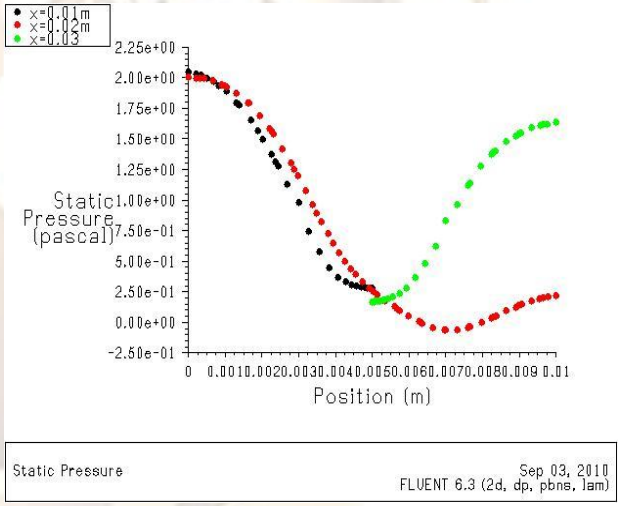

Figure 26 static pressure D=0.08cm, m=0.30kg/s

Similarly, the static pressure variation along y-direction is shown in fig. 21 to 26 The pressure drop allowance in tube bank is the static fluid pressure which drives the fluid through it. The pressure drop is greatly influenced by the spacing of the succeeding rows of tubes, their layout and closeness. From the xy-plots, it can be observed, when mass flow rate increases the pressure drop increases due to length of the recirculation zone behind the tube has an influence on pressure drop.

V NUSSELT NUMBER

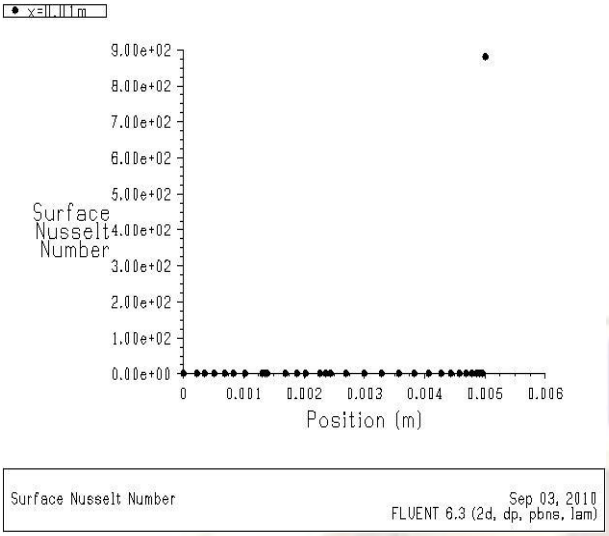

Figure 27 Nusselt number plot D=0.08cm, m=0.05kg/s

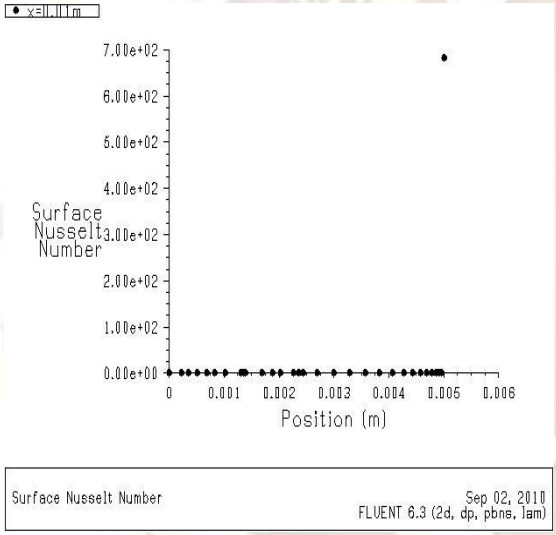

Figure 28 Nusselt number plot D= 0.08cm, m=0.10kg/s

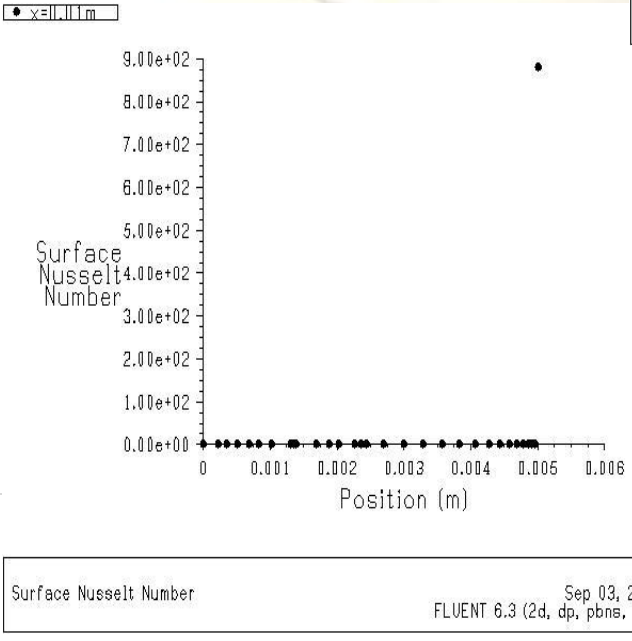

Figure 29 Nusselt number plot D=0.08cm, m=0.15kg/s

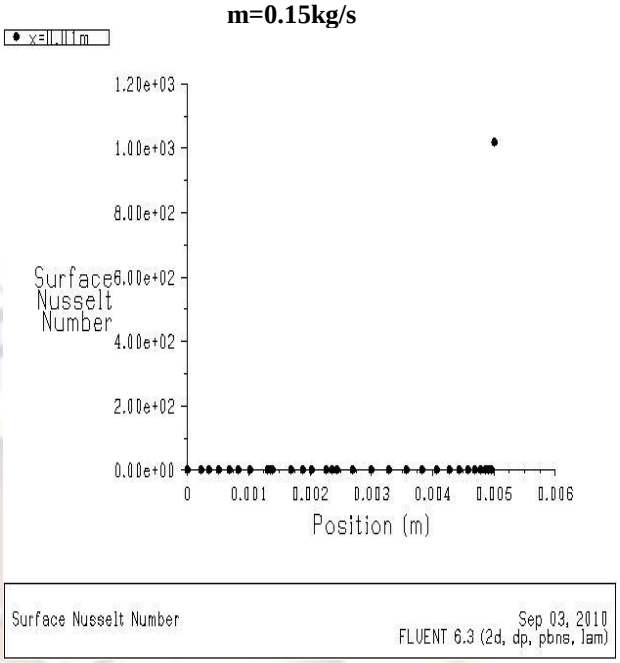

Figure 30 Nusselt number plot D=0.08cm, m=0.20kg/s

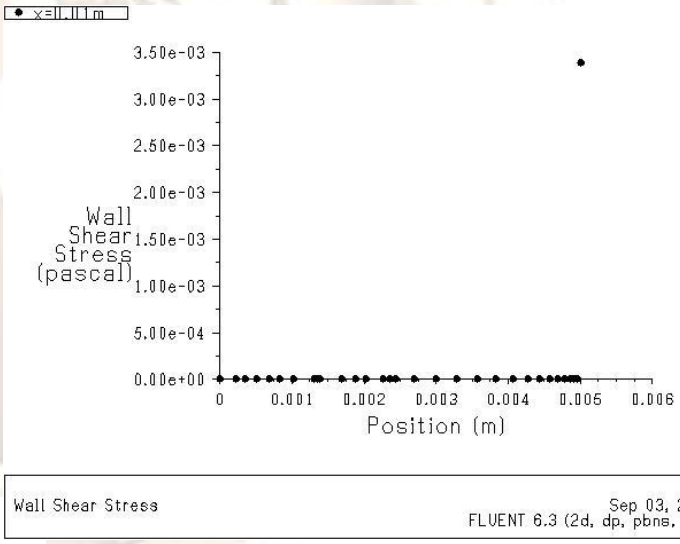

Figure 31 Nusselt number plot D=0.08cm, m=0.25kg/s

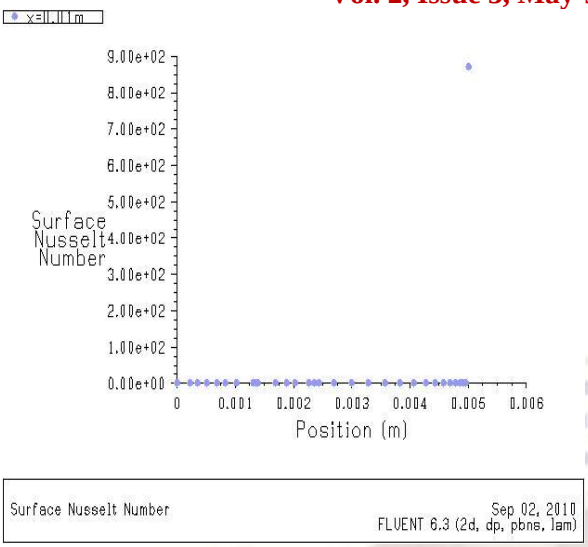

Figure 32 Nusselt number plot D=0.08cm, m=0.30kg/s

Iso-surfaces was created corresponding to the vertical cross-section through the first tube, half way between the two tubes and through the second tube. The figure 27 to 32 depicts the nusselt number on cross section of constant x-direction with the y-direction is the one which nusselt number varies. It can be observed that at the tube wall fluid attains approximately the tube wall temperature and minium at the middle of the successive rows of tube bank.

VII VERIFICATIONOF RESULTS:

The maximum velocity magnitude obtained from simulation is used to calculate the Reynolds number from the following expression,

$$Re_{Dmax}=\rho\mu_{max}D/\mu \qquad (2)$$

With the above Re_{Dmax} the Nusselt number was calculated using the correlation:

$$Nu = C1\ (C\ Re^{n}\ Pr^{0.33}) \qquad (3)$$

The total surface heat flux values obtained from the simulation was used to calculate the Nu values at x=0.01 viz., at the middle of first tube which was used to compare with correlation values. Table 5.1 presents results generated using different mass flow rates for different physical models. The results obtained from the simulation were compared to correlation results; the average error percentages for the different tube diameters are tabulated in table 5.7. It can be observed that for 1.0cm diameter of tube and 0.05kg/s of mass flow rate the average error for other the Nusselt number was 3.63% while for other p physical models with various mass flow rates the average error variation was significant. The FLUENT and correlation Nusselt number are shown in fig.

From the above simulation, the following tabular is created with different diameters, with different mass flow rates and with different tube materials we can verify the simulation results and theoretical results with the help of equation 2 and 3

For better understanding of theoretical values and simulation values for different diameters and mass flow rates, the following graphs are drawn.

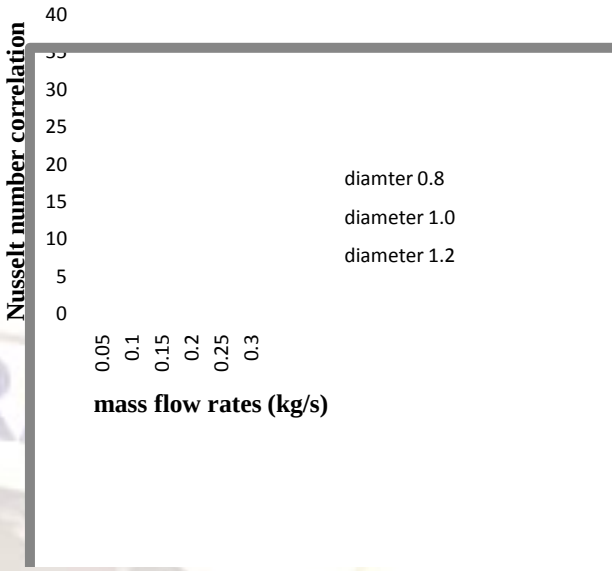

Figure 33 mass flow rates V_s Nusselt number for Aluminium tubes

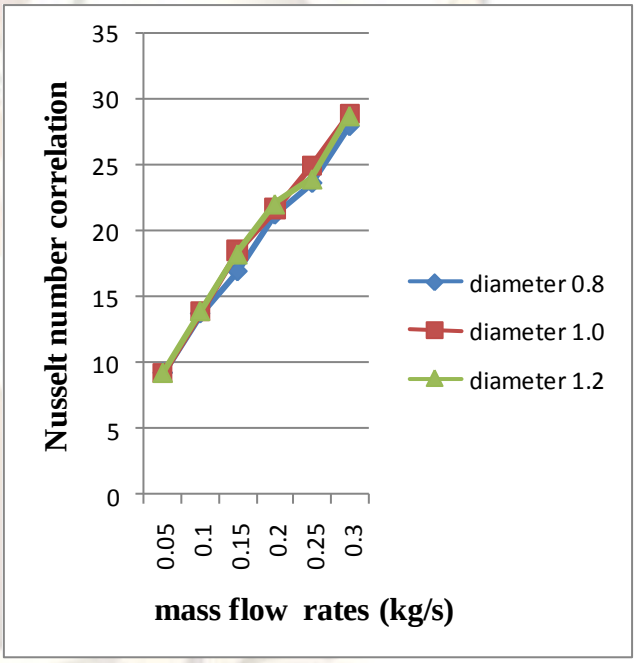

Figure 34 mass flow rate V_s Nusselt number for copper tubes.

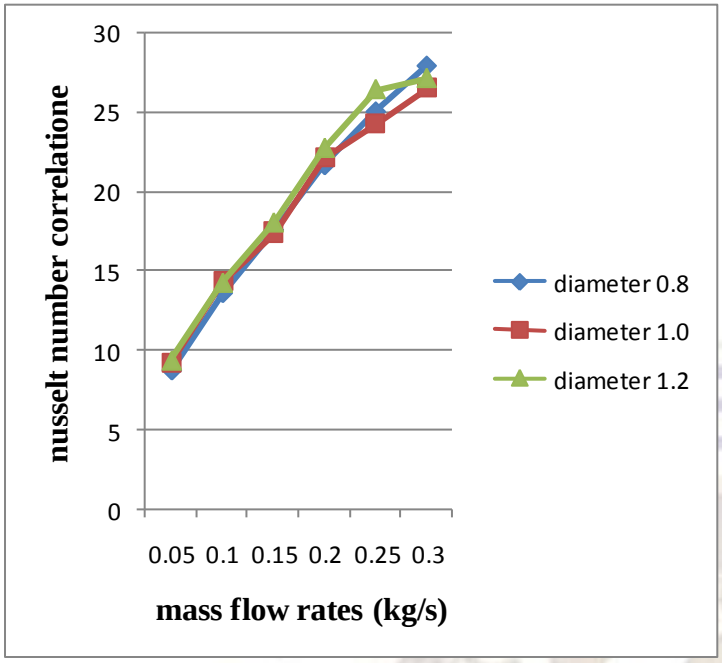

Figure 35 mass flow rate Vs nusselt number correlation for Nickel-Chromium base super alloy base tube.

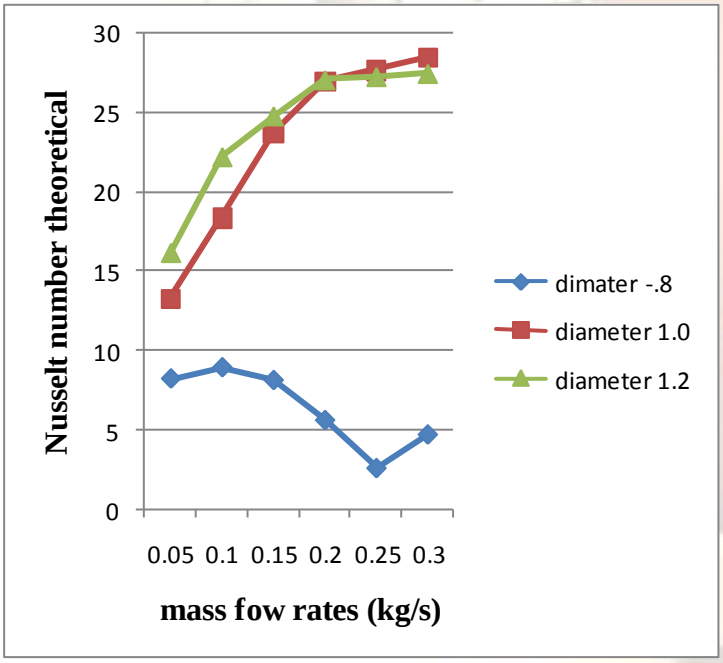

Figure 36 mass flow rate V_sNusselt number theoretical for aluminium

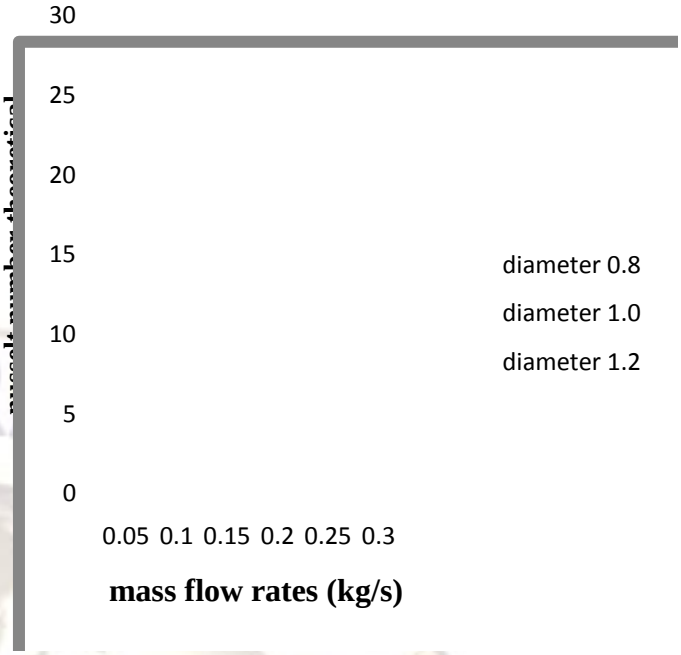

Figure 37 mass flow rates V_s Nusselt number for copper tubes.

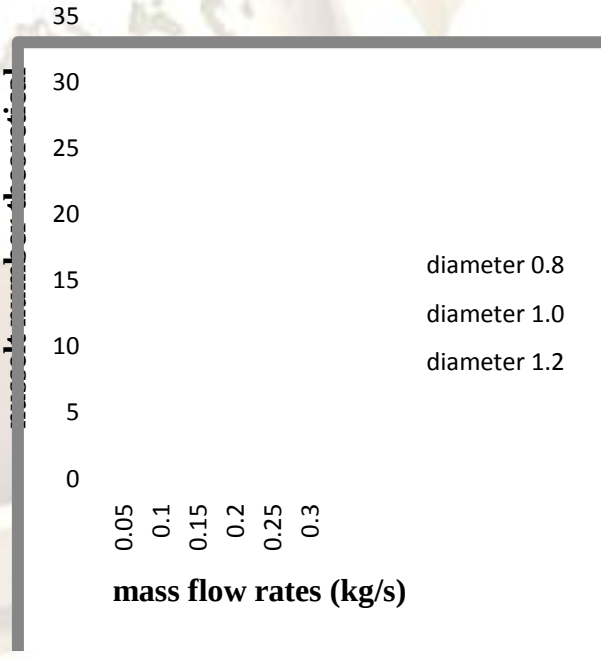

Figure 38 mass flow rates V_s nusselt number theoretical for Nickel- chromium base super alloy.

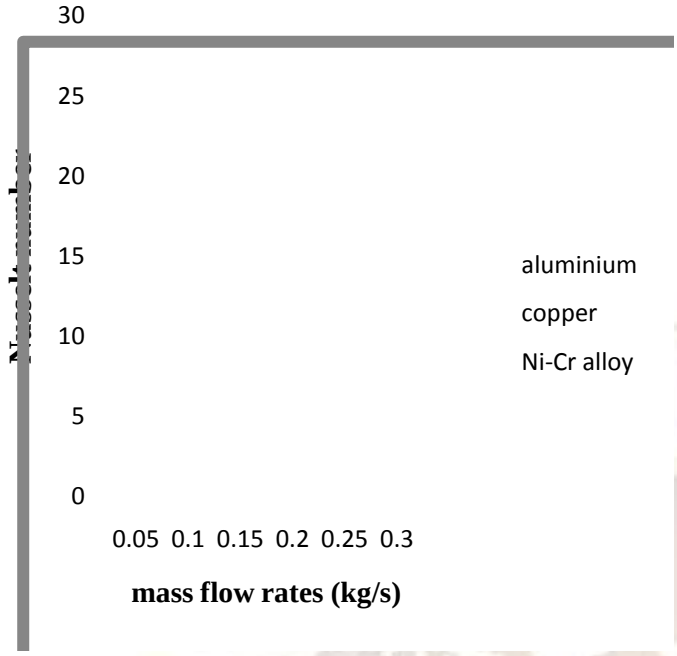

Figure 39 mass flow V_s nusselt number for different materials at d=0.08cm

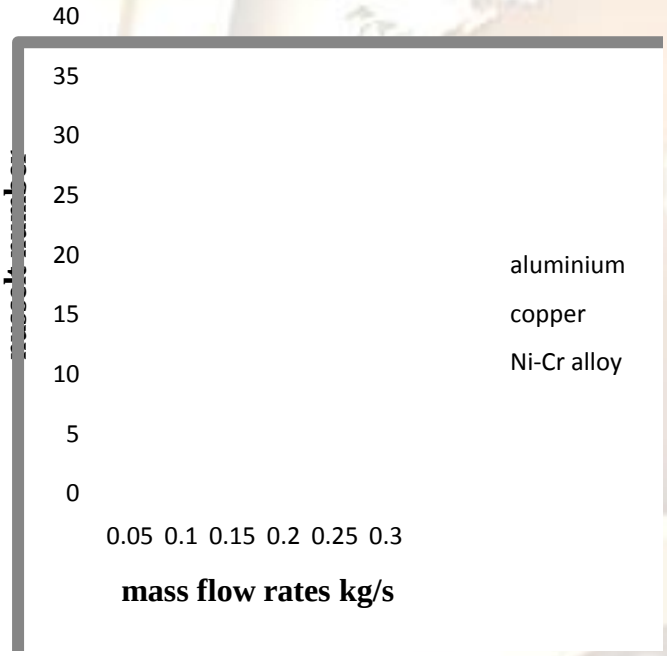

Figure 40 mass flow rates V_s nusselt number for different materials at d=1.0cm

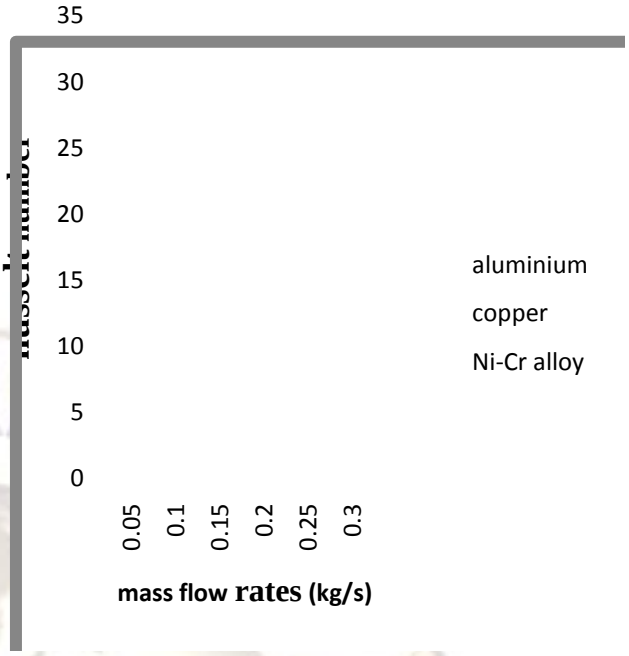

Figure 41mass flow rates Vs mass flow rates for different materials at d=1.20cm

From the above graphs the observations are:

- The effect of different mass flow rates on both flow and heat transfer is significant. It was observed that 1.0cm diameter of tubes and 0.05kg/s mass flow gives the best results as 34.30 nusselt number.
- From the above graphs we can observe that alloys serves as a better material for tube when compare with copper and aluminium.
- The effect of mass flow rates on both flow and heat transfer is significant. This is due to variation of space of the surrounding tubes.
- It was observed optimal flow distribution was found for 0.8cm diameter and 0.05kg/s mass flow rate in case of alloy.

VIII CONCLUSION

Mode and mesh creation n CFD is one of the most important phases of simulation. The model and mesh density determine the accuracy and flexibility of the simulations. Too dense a mesh will unnecessarily increase the solution time; too coarse a mesh will reach to a divergent solution quickly. But will not show an accurate flow profile. An optimal mesh is denser in areas where there are no flow profile changes.

- A two- dimensional numerical solution of flow and heat transfer in a bank of tubes which is used in industrial applications has been carried out.
- Laminar flow past a tube bank is numerically simulated in the low Reynolds number regime. Velocity vector depicts zones of recirculation between the tubes.

Nusselt number variations are obtained and pressure distribution along the bundle cross section is presented.

- The effect of different mass flow rates on both flow and heat transfer is significant. This is due to the variation of space of the succeeding rows of tubes. It was observed that 1.0cm diameter of tubes and 0.05kg/s mass flow rate gives the best results.
- Mass flow rate has an important effect to heat transfer. An optimal flow distribution can result in a higher temperature distribution and low pressure drop. It was observed that the optimal flow distribution was occurred in 1.0cm diameter and 0.05kg/s mass flow rate.
- CFD simulation are a useful tool for understanding flow and heat transfer principles as well as for modeling these types of geometries.
- It was observed that 1.0cm diameter of tubes and 0.30kg/s mass flow rate yields optimum results for aluminium as tube material, where as it was observed that 0.8cm and 0.05kg/s mass flow rate in case of copperas tube material.
- From the above graphs we observed that alloys serves as a better material for tube compared with copper and aluminium.
- Alloy (Nickel-Chromium based) serves as a better material for heat transfer applications with low cost
- Further improvements of heat transfer and fluid flow modelling can be possible by modelling three dimensional model and changing the working fluid.

REFRENCE

- Patankar, S.V. and spalding. D.B. (1974), " A calculation for the transient and steady state behaviour of shell- and- tube Heat Exchanger". Heat transfer design and theory sourcebook. Afgan A.A. and Schluner E.U.. Washington. Pp. 155-176.
- KelKar, K.M and Patankar, S. V., 1987" Numerical prediction of flow and Heat transfer in a parallel plate channel with staggered fins", Journal of Heat Transfer, vol. 109, pp 25-30.
- Berner, C., Durst, F. And McEligot, D.M., "Flow around Baffles", Journal of Heat Transfer, vol. 106 pp 743-749.
- Popiel, C.o & Vander Merwe, D.F., "Friction factor in sine-pipe flow, Journal of fluids Engineering", 118, 1996, 341-345.
- Popiel, C.O & Wojkowiak, J., "friction factor in U-type undulated pipe flow, Journal of fluids Engineering", 122, 2000, 260-263.
- Dean, W. R., Note on the motion of fluid in a curved pipe, The London, Edinburgh and Dublin philosophical Magazine, 7 (14), 1927, 208-223.
- Patankar, S.V., Liu, C.H & Sparrow, E.M., "Fully developed flow and Heat Transfer in ducts having streamwise periodic variation in cross-sectional area", Journal of Heat Transfer, 99, 1977, 180-186.
- Webb, B.W & Ramdhyani, S., "Conjugate Heat Transfer in an channel with staggered Ribs" Int. Journal of Heat and Mass Transfer 28(9), 1985,1679-1687.
- Park, K., Choi, D-H & Lee, K-s., "design optimization of plate heat exchanger with staggered pins", 14th Int. Symp.on Transport phenomena, Bali, Indonesia, 6-9 July 2003.